Journal of Bioresources and Bioproducts 6 (2021) 215–222

Contents lists available at ScienceDirect

Journal of Bioresources and Bioproducts

journal homepage: www.elsevier.com/locate/jobab

Green $CoNi_2S_4$/porphyrin decorated carbon-based nanocomposites for genetic materials detection

Mohammad Reza Saeb[a,*], Navid Rabiee[b], Farzad Seidi[c], Bahareh Farasati Far[d], Mojtaba Bagherzadeh[b], Eder C. Lima[e], Mohammad Rabiee[f]

[a] Université de Lorraine, CentraleSupélec, LMOPS, F, 57000 Metz, France
[b] Department of Chemistry, Sharif University of Technology, Tehran, Iran
[c] Provincial Key Lab of Pulp & Paper Sci and Tech, and Joint International Research Lab of Lignocellulosic Functional Materials, Nanjing Forestry University, Nanjing 210037, China
[d] Department of Chemistry, Iran University of Science and Technology, Tehran, Iran
[e] Institute of Chemistry, Federal University of Rio Grande do Sul (UFRGS), Av. Bento Goncalves 9500, Postal Box, 15003, ZIP, 91501-970 Brazil
[f] Biomaterial Group, Department of Biomedical Engineering, Amirkabir University of Technology, Tehran, Iran

ARTICLE INFO

Keywords:
Biosensor
Biomedicine
Anti-cas9
Green nanocomposite
sgRNA

ABSTRACT

A one-pot synthesis method was conceptualized and implemented to develop green carbon-based nanocomposites working as biosensors. Porphyrin was synthesized to adorn the surface of nanocomposites making them highly sensitive for giving rise to π-π interactions between the genetic materials, proteins and porphyrin rings. The hydrogen bond formed between the proteins (analytes) and the nitrogen in the porphyrin structure as well as the surface hydroxyl groups was equally probable. In this context, different forms of porphyrins were incorporated to explore the interrelationship between the surface morphology and the ability of detection of genetic material and/or proteins by the aid of the synthesized structures. This phenomenon was conceptualized to optimize the interactions between the biomolecules and the substrate by reaching significant biosensor application in the presence of Anti-cas9 protein and sgRNA (concentration changed between 10 and 500 n mol/L). Almost full quenching of fluorescence emission was observed after addition of 300 n mol/L of Anti-cas9 protein and 250 n mol/L of sgRNA. Surprisingly, $CoNi_2S_4$ provided 12%–29% cytotoxicity in both HEK-293 and PC12 cell lines.

1. Introduction

Smart selection of biomaterials governs the biological response of bio-systems (Zarrintaj et al., 2018; 2020a; 2021). Designing nanomaterials and nanosystems as sensing materials have been widely practiced in recent years (Zarrintaj et al., 2019; Rabiee et al., 2020a; Ahmadi et al., 2021b). Carbon-based nanomaterials (CNMs) are centered to the modern technologies because of their promising characteristics like high thermal and electrical conductivity as well as versatility (Khalili et al., 2020; Taghizadeh et al., 2020). The CNMs include carbon nanotubes (CNTs), graphene oxide (GO), fullerenes and nanodiamonds, black nanoparticles, carbon nanofibers, carbon nanohorns, carbon nanodots and other derivatives (Vijayan et al., 2017; Nonahal et al., 2018). The CNMs provide a wider application window rather than other non-viral vectors due to their considerable biocompatibility, affordable processing, ability to attach to both the inorganic and organic molecules, low toxicity, and high water-solubility. Reduced GO (rGO) and CNTs can interact with drugs as well as other biomolecules, such as nucleic acids, DNA and RNA (Chandrasekhar, 2018; Tong et al., 2018). Through possessing a wide sp^2-hybridized carbon area, they can make it possible to detect nucleic acids (Wang et al., 2017). Furthermore,

* Corresponding author.
E-mail address: mrsaeb2008@gmail.com (M.R. Saeb).

https://doi.org/10.1016/j.jobab.2021.06.001
Received 14 April 2021; Received in revised form 10 May 2021; Accepted 15 May 2021
Available online 8 June 2021

the aspect ratio of rGO and CNTs, i.e., the ratio of their length to their thickness or diameter, can be simply manipulated by the modification of their surface. This provides them with some advantages over other non-viral delivery systems. For instance, the CNTs have a very high length-to-diameter aspect ratio. The diameter and the length of single-walled CNTs (SWCNTs) respectively vary in the ranges of 0.4–2.5 nm and 20–1000 nm, while the aforementioned parameters vary in the range of 1.4–10 nm and 1–500 μm in the same order in multi-walled CNTs (MWCNTs).

The thermal conductivity of the CNTs varies in a wide range, from a thermal insulation level of 0.1 W/(m•K) to a thermal conductivity level of 6600 W/(m•K). Such a broad range permits to engineer the CNTs for diverse purposes. Experimentally, thermal conductivity of the individual CNTs, in kT unit, is extremely high at room temperature for MWCNTs (1400– 3000 W/(m•K)) or even much greater values for the SWCNTs. In addition, there is an electrical potential of 0.1–10 MΩ barrier (innertube junction) between the adjoining CNTs. The cohesion energy of the CNTs is 30–40 kT/nm, depending on the diameter of CNTs. Chemical GO reduction is the most frequent process for developing rGO, but it is not easy to obtain a structure with C/O ratios more than 15. For mass processing, chemical reduction is highly scalable, for reagents are cheap and readily available. The BET provided from the surface of GO is greater than that of thermally obtained rGO, while the number of structural defects is comparatively lower for GO, making it difficult to functionalize GO (its conductance spectrum is 7700–30 000 S/M) (Karimi et al., 2018; Bahrami et al., 2019; Norahan et al., 2019; Rabiee et al., 2019; Hasanzadeh et al., 2021; Zare et al., 2021).

Advances in using inorganic nanoparticles for biomedical applications are mainly devoted to development of green strategies by which one could protect the environment. This school of thought underlines the need for synthesis of green structures for biological systems based on the usage of green synthesis methods in the inert media, preferably based on green components rather than the conventional solvent-based techniques (Servatan et al., 2020; Khodadadi Yazdi et al., 2020; Zarrintaj et al., 2020b). Zinc oxide (ZnO) nanoparticles (NPs) are valuable inorganic semiconducting metal oxides as multifunctional, non-toxic, and biocompatible inorganic materials (Zamani et al., 2018). The ZnO NPs have a tremendous potential for several uses, including biosensors, diagnosis, nanomedicine, biological labels, gene delivery, pharmaceutical and drug delivery. This roots in the wide band gap (3.10–3.37 eV), large excitation binding energy (60 meV) and high piezoelectric properties of ZnO NPs (Nasseri et al., 2019; Ghadiri et al., 2020; Nik et al., 2020). The surface of ZnO or other types of zero-valent nanoparticles is chemically covered with plenty of hydroxyl groups, allowing them to dissolve slowly in almost all acidic environments. Evaluation of micro-environment of the tumor grabs a tremendous interest of scientists, where role of ZnO NPs has been extensively discussed. However, due to the intrinsic biological responses to the ZnO NPs, they are limitedly used in-vivo. To rely on this need, $CoNi_2S_4$ is developed, mostly focused on bioelectronics and supercapacitor. Recently, we succeeded in developing nanostructures based on $CoNi_2S_4$ for both the gene delivery and biosensor applications (Rabiee et al., 2016; Rabiee et al., 2020c; Rabiee et al., 2020h).

To provide design criteria for effective carbon-based device strategies, fundamental studies on the impact of the size, morphology, aggregation degree, and functional groups of CNMs are required. The specific physical properties of low-dimensional sp^2 CNMs allow for developing a wide variety of novel cancer therapies to resolve multi-drug resistance issue in current cancer chemotherapies to enhance tumor therapy effectiveness. This could be paired with therapeutic drugs and genes co-provided by the CNTs or rGO. The MWCNTs and rGO are well-known for their facile surface functionalization and also have a low toxicity among CNMs, which provides them with very reactive surface for aromatic rings acting through π-π interactions. This brings a high efficiency of drug loading due to the strong π-π stacking interactions with drugs and aromatic rings such as doxorubicin and/or genetic materials as well as the proteins (Ahmadi et al., 2020; Hajebi et al., 2020; Rabiee et al., 2020a; Rabiee et al, 2021a; Tavakolizadeh et al., 2021).

Herein, we report on the enhanced sensitivity as well as the selectivity of the aforementioned nanostructures. Correspondingly, $CoNi_2S_4$ nanoparticles were incorporated within the rGO layers, and engineered by the space through localization of MWCNTs onto the rGO layers. Creating sustainable, environmentally sensitive nanosystems may lead to innovative ways for early diagnosis and detection of different kinds of disease. Meanwhile, the use of systems that can be optimized in several different applications is responsible for a significant cost reduction, enhanced sensitivity as well as exceptional selectivity. To date, various studies on the early detection of diseases have been performed based on various biomarkers, mainly based on electrochemical sensing methods, but they suffer from high costs and difficulty with optimization (Nour et al., 2019; Rabiee et al., 2020j). In this study, for the first time, we focused on design, synthesis and characterization of one-pot green synthesized carbon-based nanocomposites in the presence of nickel and cobalt, and modified them with porphyrin molecules to make the nanocomposite sensitive to genetic materials and proteins. The synthesized porphyrin molecules can act as biodegradable, biocompatible and natural components to reduce the potential cytotoxicity of toxic elements.

2. Materials and methods

2.1. Materials

The graphitic powder, potassium permanganate ($KMnO_4$), sulfuric acid (H_2SO_4, 98%), $Ni(NO_3)_2$•$6H_2O$, $Co(NO_3)_2$•$6H_2O$, hydrochloric acid (HCl, 36%), hydrogen peroxide (H_2O_2, 30% V/V), multiwalled carbon nanotubes (MWCNTs, purity > 90%, length < 9 μm and OD = 10–20 nm), mesitaldehyde, DDQ, and sodium acetate anhydrous (NaAc) were all procured from Sigma-Aldrich, Germany. All of the solvents were used of HPLC grade.

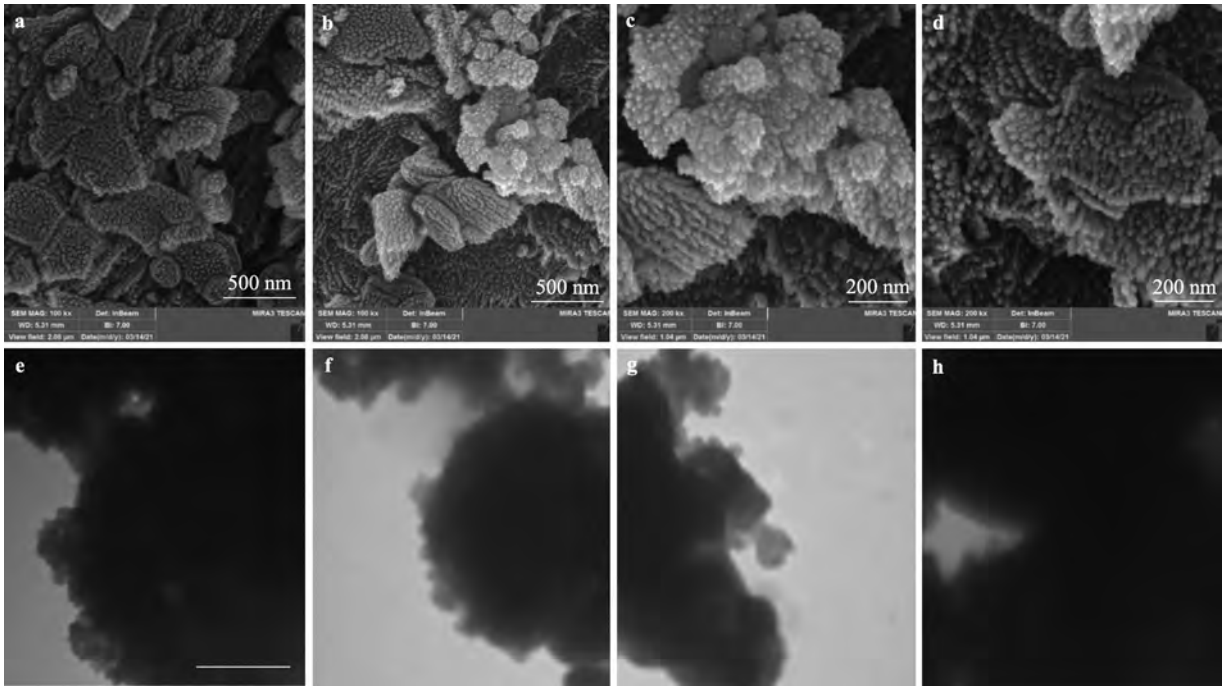

Fig. 1. Field-Emission Scanning Electron Microscope (FESEM) (a, b, c and d) and Transmission Electron Microscopy (TEM) (e, f, g and h) results on the synthesized nanocomposite (rGO/MWCNT/$CoNi_2S_4$) showed the $CoNi_2S_4$ nanoparticles decorated on the surface, and the lamellar rGO sheets along with the aggregated multi-walled carbon nanotubes (MWCNTs). Scale bar of TEM is 100 nm.

2.2. One-pot and green synthesis of nanocomposite

Nanocomposite based on rGO, MWCNT and $CoNi_2S_4$ was prepared via a one-pot and green procedure. The protocol is available in a previous work of this group (Rabiee et al., 2021b). Briefly, MWCNT (100 mg) and rGO (200 mg) were dispersed in 100 mL of ethylene glycol. Then, a solution of IPA/water (1:1) (110 mL) was added and stirred for 5 h, at ambient temperature. In the next step, 2 mmol of $Ni(NO_3)_2$•$6H_2O$ and 1 mmol of $Co(NO_3)_2$•$6H_2O$ along with 9 mmol of thiourea were poured into the solution, and stirred for about 1 h, at ambient temperature.

2.3. Synthesis of porphyrin (H_2TMP)

Detailed synthesis of the porphyrin can be found in a previous work (Rabiee et al., 2021c). For the synthesis of H_2TMP, 10 mmol mesitaldehyde and 10 mmol distilled pyrrole were added to 100 mL of chloroform. The solution was then stirred for 10 min and purged with the N_2. Then, 3.3 mmol of boron trifluoride-diethyl ether (10^{-3} M) was added to the reaction mixture via a syringe. The solution was stirred at room temperature for 1 h and oxidized with excess amount of 1,2-dichloro 4,5-dicyanoquinone (DDQ), followed by absorption spectrophotometry. Next, 7.5 mmol of *p*-chloranil was added to the reaction mixture and refluxed for 1 h. Finally, the reaction mixture was cooled to room temperature and 3.3 mmol of trimethylamine was added followed by removal of solvent on a rotary evaporator. The product was washed for several times by ultrapure water and methanol and stored.

2.4. Fabrication of nanomaterial for biomedical assays

In order to prepare the suitable nanomaterial for biomedical assay, the synthesized H_2TMP (12 mg) was dispersed into N, N-dimethylformamide (DMF) (40 mL) and sonicated in a dark place for 17 min, and then the synthetic nanocomposite (20 mg) was added to the mixture. The final mixture was stirred for 24 h in a dark place at room temperature.

2.5. MTT assays

In order to analyze the cytocompatibility of the prepared nanomaterials, (3-[4,5-dimethylthiazol-2-yl]-2,5-diphenyltetrazolium bromide) (MTT, Sigma) assay was performed based on the literature (Rabiee et al., 2020f). Two cell lines, PC12 cells (ATCC CRL-1721^{TM}) and HEK-293 (ATCC CRL-1721^{TM}), were correspondingly applied. In this manner, 1×10^5 cells per well were cultured in the presence of the prepared nanomaterials, and the used microenvironment was based on Dulbecco's Modified Eagle's Medium (DMEM,

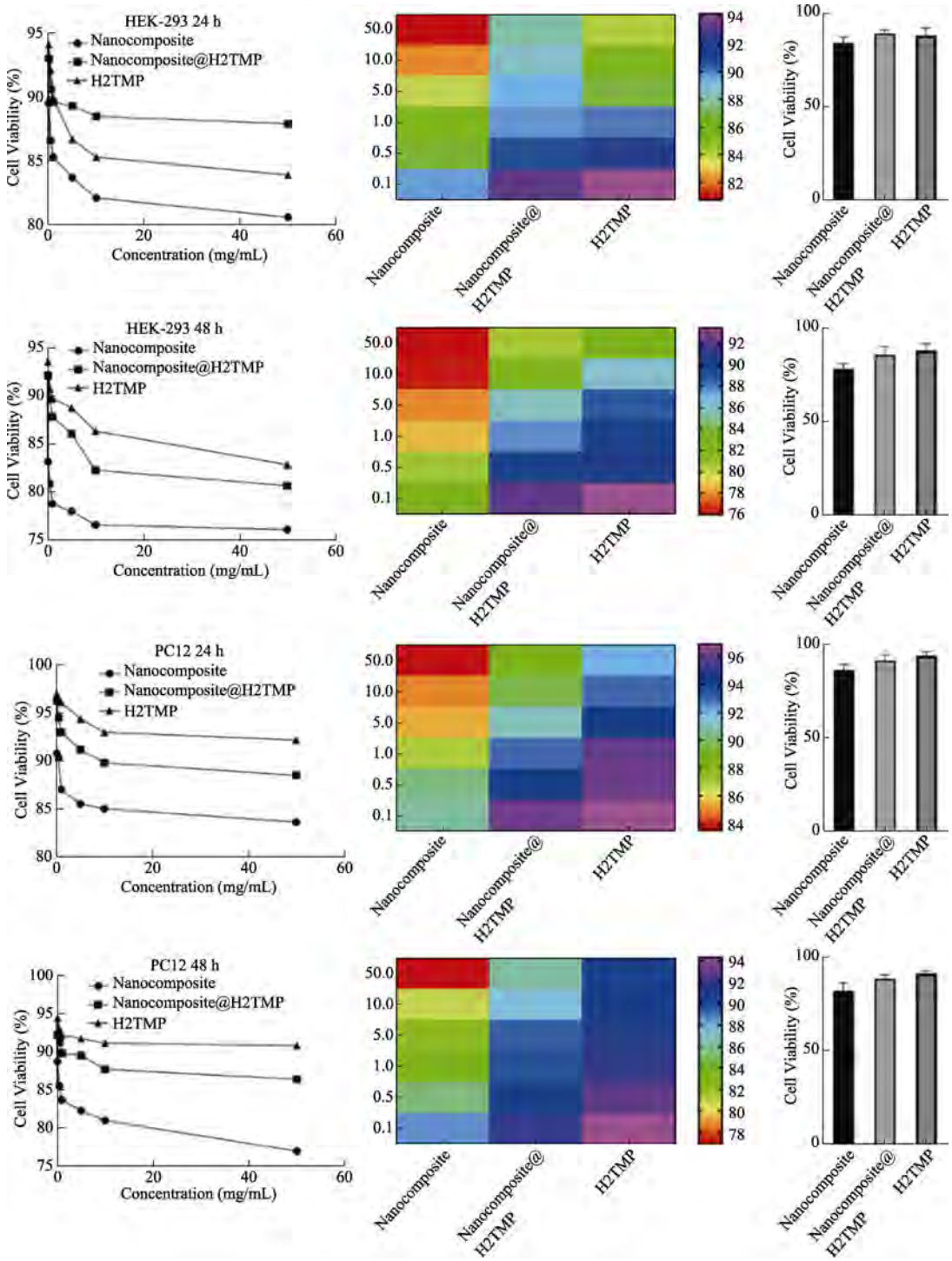

Fig. 2. Results of the MTT assays on the HEK-293 and PC12 cell lines after 24 and 48 h of treatment. The first column is the dose-dependent MTT assays results. The second column is the heat map of the dose-dependent MTT assay results; and the third column is the median value of relative cell viability.

Table 1
Different nanomaterials developed and applied for optical biosensors based on DNA and comparison with results of the current work.

Probe	Detection element	MQE (%)	LOD	Detection range	Donor (excitation/emission) (nm)	Reference
ssDNA	*Staphylococcus aureus* DNA	90	0.0062 nM	0.0125 – 3.12 nM	FITC, 480/520	(Pang et al., 2013)
ssDNA	A special form of DNA	100	0.5 pM	2 pM–1 nM	FITC and TAMAR 488, 543/516	(Peng et al., 2012)
ssDNA	A special form of DNA	–	20 pM	50 pM–100 nM	FAM, 494/518	(Zhao et al., 2012)
ssDNA	A special form of DNA	94	34 pM	0.1– 3 nM	CL	(Luo et al., 2012)
ssDNA	A special form of DNA	100	0.25 pM	0–10 nM	SG, -/530	(Li et al., 2013)
ssDNA	A special form of DNA	96	0.31 pM	0.5–100 nM	SG, 490/529	(Zhang et al., 2011)
ssDNA	Exonuclease activity and DNA sequence	91	32 nM	50–2500 nM	EB, 480/605	(Jiang et al., 2013)
ssDNA	Hybridization of DNA	95	200 nM	–	GO, 400/547	(Liu et al., 2010)
Nano-beacon probe based on hairpin structures	Activity of T4 polynucleotide	100	0.001 U/mL	0–0.3 U/mL	FAM, 494/525	(Wu et al., 2011)
Probe based on molecular beacon	DNA damage	94	0.2 nM	0.8–50 nM	FAM, 480/517	(Zhao et al., 2012)
Synthesized nanocomposite (rGO/MWCNT/$CoNi_2S_4$/H_2TMP)	Anti-cas9 protein; sgRNA	–	10 nM	10–500 nM	Porphyrin (H_2TMP)	This work

Notes: MQE, maximum quenching efficiency; LOD, limit of detection.

Gibco), which contained fetal bovine serum, streptomycin and penicillin in a normal and standard volumes. Then, the prepared cells were incubated at 37 °C and 5% CO_2. Afterwards, a determined concentration of MTT solution (5 mg/mL) was added to each well, and incubated for four hours. In the next step, the final medium was removed and the formazone precipitates were dissolved in dimethyl sulfoxide (DMSO; Sigma-Aldrich,). The optical absorbance was measured at 570 nm using a microplate Elisa reader (ELX808, BioTek).

2.6. Genetic material interaction investigations

In order to analyze the possible interaction between the anti-cas9 and sgRNA and the synthesized nanomaterials, an exact concentration of the nanomaterials (200 μL in volume with the concentration of 14 mg/mL) and 33 μL of the genetic material (protein) were incubated at 37 °C for 50 min. Then, in order to remove the surface adsorbed genetic material (protein), the nanomaterials were centrifuged at 8000 r/min for 20 min. All of these steps were repeated with different concentrations of the nanomaterials and the genetic materials (protein), in order to analyze the exact mechanism as well as the potentials in sensing the genetic material with different weight ratios (WR's).

3. Results and discussion

In order to analyze the successful synthesis of the nanomaterials, a low-cost, fast, reliable and available analysis was conducted. In this manner, based on our previous works (Rabiee et al., 2020f; 2020g; 2021b; 2021c), full morphological analysis was carried out using Field-Emission Scanning Electron Microscope (FESEM) and Transmission Electron Microscopy (TEM) as reliable and important tests for biomedical applications. Based on our previous works, the synthesized nanomaterials based on the rGO layers and MWCNT have similar structures (Fig. 1) to the literature, which means successful synthesis of these nanocomposites. In addition, in the TEM images (Figs. 1e, 1f, 1g and 1h), carbonic layers showed clearly in the presence of cone-shape $CoNi_2S_4$ nanoparticles. This study was designed based on the using low-cost methods for both of the preparation and application; therefore, it is not necessary to perform high-cost time-consuming characterizations.

In order to evaluate the biocompatibility and relative cell viability of the synthesized nanocomposite, with and without the porphyrin, MTT assays on the HEK-293 and PC12 cell lines were conducted after 24 and 48 h of treatment. The results (Fig. 2) showed that by addition of porphyrin to the nanostructures, the relative cell viability increased in all cases, suggesting that the porphyrin could act as natural polymers like chitosan and alginate (Rabiee et al., 2020i; Kiani et al., 2021). These natural polymers are able to inhibit the cellular interaction between the toxic elements like cobalt and nickel and the microenvironments, leading to increasing in the relative cell viability in the range of 5%–24% (Kiani et al., 2020; Maghsoudi et al., 2020; Rabiee et al., 2020d; Bagherzadeh et al., 2021). The heat map of relative cell viability showed clearly that by incorporation of the free-standing nanocomposites to the cell wells, the relative cell viability is in the worst situation compared with the free porphyrin and porphyrin decorated nanocomposite. These results emphasize on the role of $CoNi_2S_4$ in providing 12%–29% cytotoxicity in both of the HEK-293 and PC12 cell lines. Therefore, the role of porphyrin in this work as a sensitizer for the optical detection of genetic materials and proteins changes, and turns to an inhibitor of interactions with the cellular membranes.

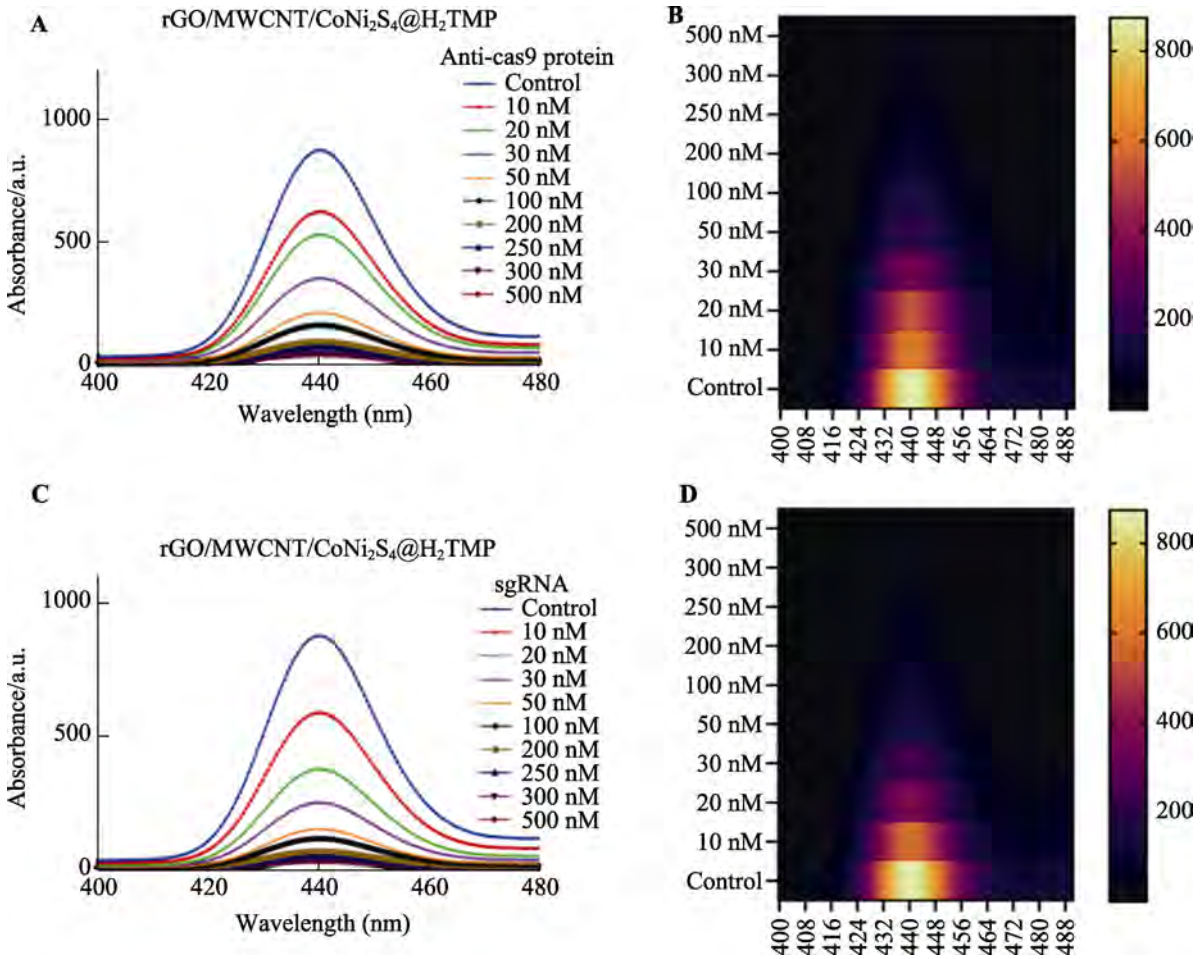

Fig. 3. Fluorescence emission spectra of synthesized nanomaterial in the presence of Anti-cas9 protein and sgRNA.

The sensitivity of the prepared nanocomposite decorated with the porphyrin was investigated in the presence of different concentrations of Anti-cas9 protein and sgRNA. Both of these proteins and genetic materials are able to have physical and spatial interactions with the synthesized nanocomposite, which resulted in quenching in the fluorescence emission spectra of the porphyrins (Nasseri et al., 2018; Toudeshkchoui et al., 2019; Rabiee et al., 2020b; Rabiee et al., 2020e). Also, these proteins could have stable chemical interactions with the amino acid domains, leading to stable and steady decreasing in the fluorescence emission spectra (Ghasemi et al., 2018; Parsa et al., 2018; Vafajoo et al., 2018; Ahmadi et al., 2021a; Rabiee et al., 2020k). In this study, the optical relationship between the synthesized nanocomposite and 10–500 n mol/L concentrations of Anti-cas9 protein and sgRNA were screened. Based on the results (Fig. 3), by increasing the concentration of Anti-cas9 protein from 10–20 n mol/L, no significant decrease in the fluorescence emission was observed. However, by increasing the concentration of Anti-cas9 protein to over 50 n mol/L, almost 70% of the fluorescence emission was quenched successfully, which could be considered as a promising biosensor for the detection of Anti-cas9 protein with trance concentrations. In case of sgRNA, by increasing the concentration of sgRNA up to 50 n mol/L, almost 80% of the fluorescence emission was quenched, which in comparison to the Anti-cas9 protein, leading to more promising results. Almost full quenching of fluorescence emission was observed after addition of 300 n mol/L of Anti-cas9 protein and 250 n mol/L of sgRNA. Regarding the selectivity of these nanocomposites, it should be noted that these analytes can not present in the blood and/or plasma sample of a single patient (Crudele and Chamberlain, 2018; Johnston et al., 2019; Osuna et al., 2020). Therefore, there is no competition between these analytes. Also, based on the literature (Bondy-Denomy, 2018; Galizi and Jaramillo, 2019; Zhang et al., 2020), there are limited works with promising results based on the analytes due to their special functionality as well as the morphology; but, this study showed that a green, cost-effective and non-purified nanocomposite could be able to detect the trace concentrations of these analytes successfully. Based on the literature (Table 1), both the limit of detection (LOD) and detection range of the results of this study were considered in the range of applicable and were promising. There are some more favorable results regarding the detection of ordinary DNA-type analytes in the literature, but till now, there is no report on the use of simple, green and cost-effective nanocomposite for the detection of Anti-cas9 and sgRNA.

4. Conclusions

In this work, a simple, cost-effective, green and adjustable method for preparation of a routine and simple nanocomposite based on rGO/MWCNT/$CoNi_2S_4$ was designed. After that, a simple method was applied based on the morphological analysis for performance analysis. In the next step, a sensitive molecule, porphyrin, in a rigid form was designed and synthesized, and decorated on the surface of the synthesized nanocomposite. The porphyrin would be able to make any nanostructures very sensitive to any analytes, with its own great fluorescence emission. However, the concept of this work was to localize the porphyrins inside the porosity of the nanocomposite in order to optically detect the anti-cas9 and sgRNA and their nucleotides (compartments) selective with the LOD of below 10 n mol/L and the range of detection of 10–500 n mol/L.

Declaration of Competing Interest

The authors declare no competing interest.

References

Ahmadi, S., Rabiee, N., Bagherzadeh, M., Karimi, M., 2021a. Microfluidic devices for pathogen detection. Biomedical Applications of Microfluidic Devices. Elsevier, Amsterdam, pp. 117–151.

Ahmadi, S., Rabiee, N., Fatahi, Y., Bagherzadeh, M., Gachpazan, M., Baheiraei, N., Nasseri, B., Karimi, M., Webster, T.J., Hamblin, M.R., 2020. Controlled gene delivery systems: nanomaterials and chemical approaches. J. Biomed. Nanotechnol. 16, 553–582.

Ahmadi, S., Rabiee, N., Fatahi, Y., Hooshmand, S.E., Bagherzadeh, M., Rabiee, M., Jajarmi, V., Dinarvand, R., Habibzadeh, S., Saeb, M.R., Varma, R.S., Shokouhimehr, M., Hamblin, M.R., 2021b. Green chemistry and coronavirus. Sustain. Chem. Pharm. 21, 100415.

Bagherzadeh, M., Rabiee, N., Fatahi, Y., Dinarvand, R., 2021. Zn-rich $(GaN)_{1-x}(ZnO)x$: a biomedical friend? New J. Chem. 45, 4077–4089.

Bahrami, S., Baheiraei, N., Mohseni, M., Razavi, M., Ghaderi, A., Azizi, B., Rabiee, N., Karimi, M., 2019. Three-dimensional graphene foam as a conductive scaffold for cardiac tissue engineering. J. Biomater. Appl. 34, 74–85.

Bondy-Denomy, J., 2018. Protein inhibitors of CRISPR-cas9. ACS Chem. Biol. 13, 417–423.

Chandrasekhar, P., 2018. CNT applications in drug and biomolecule delivery. Conduct. Polym. Fundam. Appl. 61–64.

Crudele, J.M., Chamberlain, J.S., 2018. Cas9 immunity creates challenges for CRISPR gene editing therapies. Nat. Commun. 9, 1–3.

Galizi, R., Jaramillo, A., 2019. Engineering CRISPR guide RNA riboswitches for in vivo applications. Curr. Opin. Biotechnol. 55, 103–113.

Ghadiri, A.M., Rabiee, N., Bagherzadeh, M., Kiani, M., Fatahi, Y., Di Bartolomeo, A., Dinarvand, R., Webster, T.J., 2020. Green synthesis of CuO- and Cu_2O-NPs in assistance with high-gravity: the flowering of nanobiotechnology. Nanotechnology 31, 425101.

Ghasemi, A., Rabiee, N., Ahmadi, S., Hashemzadeh, S., Lolasi, F., Bozorgomid, M., Kalbasi, A., Nasseri, B., Shiralizadeh Dezfuli, A., Aref, A.R., Karimi, M., Hamblin, M.R., 2018. Optical assays based on colloidal inorganic nanoparticles.. Anal 143, 3249–3283.

Hajebi, S., Mohammadi Nasr, S., Rabiee, N., Bagherzadeh, M., Ahmadi, S., Rabiee, M., Tahriri, M., Tayebi, L., Hamblin, M.R., 2020. Bioresorbable composite polymeric materials for tissue engineering applications. Int. J. Polym. Mater. Polym. Biomater. 1–15.

Hasanzadeh, A., Jahromi, M.A.M., Abdoli, A., Mohammad-Beigi, H., Fatahi, Y., Nourizadeh, H., Rabiee, N., 2021. Photoluminescent carbon quantum dot/poly-L-Lysine core-shell nanoparticles: a novel candidate for gene delivery. J. Drug Delivery Sci. Technol. 61, 102118.

Jiang, Y.X., Tian, J.N., Chen, S., Zhao, Y.C., Wang, Y., Zhao, S.L., 2013. A graphene oxide-based sensing platform for the label-free assay of DNA sequence and exonuclease activity via long range resonance energy transfer. J. Fluoresc. 23, 697–703.

Johnston, R.K., Seamon, K.J., Saada, E.A., Podlevsky, J.D., Branda, S.S., Timlin, J.A., Harper, J.C., 2019. Use of anti-CRISPR protein AcrIIA4 as a capture ligand for CRISPR/Cas9 detection. Biosens. Bioelectron. 141, 111361.

Karimi, M., Mansouri, M.R., Rabiee, N., Hamblin, M.R., 2018. Carbon-based nanomaterials. Advances in Nanomaterials for Drug Delivery: Polymeric, Nanocarbon and Bio-inspired. IOP Publishing, Bristol.

Khalili, R., Zarrintaj, P., Jafari, S.H., Vahabi, H., Saeb, M.R., 2020. Electroactive poly (p-phenylene sulfide)/r-graphene oxide/chitosan as a novel potential candidate for tissue engineering. Int. J. Biol. Macromol. 154, 18–24.

Khodadadi Yazdi, M., Zarrintaj, P., Hosseiniamoli, H., Mashhadzadeh, A.H., Saeb, M.R., Ramsey, J.D., Ganjali, M.R., Mozafari, M., 2020. Zeolites for theranostic applications. J. Mater. Chem. B 8, 5992–6012.

Kiani, M., Bagherzadeh, M., Kaveh, R., Rabiee, N., Fatahi, Y., Dinarvand, R., Jang, H.W., Shokouhimehr, M., Varma, R.S., 2020. Novel Pt-Ag_3PO_4/CdS/chitosan nanocomposite with enhanced photocatalytic and biological activities. Nanomaterials 10, 2320.

Kiani, M., Rabiee, N., Bagherzadeh, M., Ghadiri, A.M., Fatahi, Y., Dinarvand, R., Webster, T.J., 2021. Improved green biosynthesis of chitosan decorated Ag- and Co_3O_4-nanoparticles: a relationship between surface morphology, photocatalytic and biomedical applications. Nanomed.: Nanotechnol. Biol. Med. 32, 102331.

Li, J., Huang, Y., Wang, D.F., Song, B., Li, Z.H., Song, S.P., Wang, L.H., Jiang, B.W., Zhao, X.C., Yan, J., Liu, R., He, D.N., Fan, C.H., 2013. A power-free microfluidic chip for SNP genotyping using graphene oxide and a DNA intercalating dye. Chem. Commun. 49, 3125.

Liu, F., Choi, J.Y., Seo, T.S., 2010. Graphene oxide arrays for detecting specific DNA hybridization by fluorescence resonance energy transfer. Biosens. Bioelectron. 25, 2361–2365.

Luo, M., Chen, X., Zhou, G.H., Xiang, X., Chen, L., Ji, X.H., He, Z.K., 2012. Chemiluminescence biosensors for DNA detection using graphene oxide and a horseradish peroxidase-mimicking DNAzyme. Chem. Commun. 48, 1126–1128.

Maghsoudi, S., Taghavi Shahraki, B., Rabiee, N., Fatahi, Y., Dinarvand, R., Tavakolizadeh, M., Ahmadi, S., Rabiee, M., Bagherzadeh, M., Pourjavadi, A., Farhadnejad, H., Tahriri, M., Webster, T.J., Tayebi, L., 2020. Burgeoning polymer nano blends for improved controlled drug release: a review. Int. J. Nanomed. 15, 4363–4392.

Nasseri, B., Kocum, I.C., Seymen, C.M., Rabiee, N., 2019. Penetration depth in nanoparticles incorporated radiofrequency hyperthermia into the tissue: comprehensive study with histology and pathology observations. IET Nanobiotechnol. 13, 634–639.

Nasseri, B., Soleimani, N., Rabiee, N., Kalbasi, A., Karimi, M., Hamblin, M.R., 2018. Point-of-care microfluidic devices for pathogen detection. Biosens. Bioelectron. 117, 112–128.

Nik, A.B., Zare, H., Razavi, S., Mohammadi, H., Ahmadi, P.T., Yazdani, N., Mobarakeh, J.I., 2020. Smart drug delivery: capping strategies for mesoporous silica nanoparticles. Microporous Mesoporous Mater. 299, 110115.

Nonahal, M., Rastin, H., Saeb, M.R., Sari, M.G., Moghadam, M.H., Zarrintaj, P., Ramezanzadeh, B., 2018. Epoxy/PAMAM dendrimer-modified graphene oxide nanocomposite coatings: nonisothermal cure kinetics study. Prog. Org. Coat. 114, 233–243.

Norahan, M.H., Amroon, M., Ghahremanzadeh, R., Rabiee, N., Baheiraei, N., 2019. Reduced graphene oxide: osteogenic potential for bone tissue engineering. IET Nanobiotechnology 13, 720–725.

Nour, S., Baheiraei, N., Imani, R., Rabiee, N., Khodaei, M., Alizadeh, A., Moazzeni, S.M., 2019. Bioactive materials: a comprehensive review on interactions with biological microenvironment based on the immune response. J. Bionic Eng. 16, 563–581.

Osuna, B.A., Karambelkar, S., Mahendra, C., Sarbach, A., Johnson, M.C., Kilcher, S., Bondy-Denomy, J., 2020. Critical anti-CRISPR locus repression by a Bi-functional Cas9 inhibitor. Cell Host Microbe 28, 23–30.

Pang, S., Gao, Y., Li, Y., Liu, S.Y., Su, X.G., 2013. A novel sensing strategy for the detection of *Staphylococcus aureus* DNA by using a graphene oxide-based fluorescent probe. Anal 138, 2749.

Parsa, S.F., Vafajoo, A., Rostami, A., Salarian, R., Rabiee, M., Rabiee, N., Rabiee, G., Tahriri, M., Yadegari, A., Vashaee, D., Tayebi, L., Hamblin, M.R., 2018. Early diagnosis of disease using microbead array technology: a review. Anal. Chimica Acta 1032, 1–17.
Peng, L., Zhu, Z., Chen, Y., Han, D., Tan, W.H., 2012. An exonuclease III and graphene oxide-aided assay for DNA detection. Biosens. Bioelectron. 35, 475–478.
Rabiee, M., Rabiee, N., Salarian, R., Rabiee, G., 2019. Bio-inspired approaches: carbon-based nanomaterials. Introduction to Nanomaterials in Medicine. IOP Publishing, Bristol.
Rabiee, N., Ahmadi, S., Afshari, R., Khalaji, S., Rabiee, M., Bagherzadeh, M., Fatahi, Y., Dinarvand, R., Tahriri, M., Tayebi, L., Hamblin, M.R., Webster, T.J., 2021a. Polymeric nanoparticles for nasal drug delivery to the brain: relevance to Alzheimer's disease. Adv. Therap. 4, 2000076.
Rabiee, N., Ahmadi, S., Arab, Z., Bagherzadeh, M., Safarkhani, M., Nasseri, B., Rabiee, M., Tahriri, M., Webster, T.J., Tayebi, L., 2020a. Aptamer hybrid nanocomplexes as targeting components for antibiotic/gene delivery systems and diagnostics: a review. Int. J. Nanomed. 15, 4237–4256.
Rabiee, N., Ahmadi, S., Fatahi, Y., Rabiee, M., Bagherzadeh, M., Dinarvand, R., Webster, T.J., 2020b. Nanotechnology-assisted microfluidic systems: from bench to bedside. Nanomedicine 16, 237–258.
Rabiee, N., Bagherzadeh, M., Ghadiri, A.M., Fatahi, Y., Baheiraei, N., Safarkhani, M., Aldhaher, A., Dinarvand, R., 2021b. Bio-multifunctional noncovalent porphyrin functionalized carbon-based nanocomposite. Sci. Rep. 11, 6604.
Rabiee, N., Bagherzadeh, M., Ghadiri, A.M., Kiani, M., Aldhaher, A., Ramakrishna, S., Tahriri, M., Tayebi, L., Webster, T.J., 2020c. Green synthesis of ZnO NPs via *Salvia hispanica*: evaluation of potential antioxidant, antibacterial, mammalian cell viability, H1N1 influenza virus inhibition and photocatalytic activities. J. Biomed. Nanotechnol. 16, 456–466.
Rabiee, N., Bagherzadeh, M., Ghadiri, A.M., Kiani, M., Webster, T.J., 2020d. High-gravity-assisted green synthesis of NiO-NPs anchored on the surface of biodegradable nanobeads with potential biomedical applications. J. Biomed. Nanotechnol. 16, 520–530.
Rabiee, N., Bagherzadeh, M., Ghadiri, A.M., Salehi, G., Fatahi, Y., Dinarvand, R., 2020e. ZnAl nano layered double hydroxides for dual functional CRISPR/Cas9 delivery and enhanced green fluorescence protein biosensor. Sci. Rep. 10, 20672.
Rabiee, N., Bagherzadeh, M., Heidarian Haris, M., Ghadiri, A.M., Matloubi Moghaddam, F., Fatahi, Y., Dinarvand, R., Jarahiyan, A., Ahmadi, S., Shokouhimehr, M., 2021c. Polymer-coated NH_2-UiO-66 for the codelivery of DOX/pCRISPR. ACS Appl. Mater. Interfaces 13, 10796–10811.
Rabiee, N., Bagherzadeh, M., Kiani, M., Ghadiri, A.M., 2020f. *Rosmarinus officinalis* directed palladium nanoparticle synthesis: investigation of potential anti-bacterial, anti-fungal and Mizoroki-Heck catalytic activities. Adv. Powder Technol. 31, 1402–1411.
Rabiee, N., Bagherzadeh, M., Kiani, M., Ghadiri, A.M., Etessamifar, F., Jaberizadeh, A.H., Shakeri, A., 2020g. Biosynthesis of copper oxide nanoparticles with potential biomedical applications. Int. J. Nanomed. 15, 3983–3999.
Rabiee, N., Bagherzadeh, M., Kiani, M., Ghadiri, A.M., Zhang, K.Q., Jin, Z., Ramakrishna, S., Shokouhimehr, M., 2020h. High gravity-assisted green synthesis of ZnO nanoparticles via *Allium ursinum*: conjoining nanochemistry to neuroscience. Nano Express 1, 020025.
Rabiee, N., Bagherzadeh, M., Tavakolizadeh, M., Pourjavadi, A., Atarod, M., Webster, T.J., 2020i. Synthesis, characterization and mechanistic study of nano chitosan tetrazole as a novel and promising platform for CRISPR delivery. Int. J. Polym. Mater. Polym. Biomater. 1–11.
Rabiee, N., Hajebi, S., Ahmadi, S., Rabiee, M., Bagherzadeh, M., Maghsoudi, S., Hamblin, M.R., 2020j. Protein microarrays: conclusions and future perspectives. Protein and Peptide-based Microarrays for Multiplex Detection, p. 1.
Rabiee, N., Karimi, M., Hamblin, M., 2016. Polymeric and hyper-branched nanoparticles and dendrimers. Advances in Nanomaterials for Drug Delivery. IOP Publishing, Bristol.
Rabiee, N., Yaraki, M.T., Garakani, S.M., Garakani, S.M., Ahmadi, S., Lajevardi, A., Bagherzadeh, M., Rabiee, M., Tayebi, L., Tahriri, M., Hamblin, M.R., 2020k. Recent advances in porphyrin-based nanocomposites for effective targeted imaging and therapy. Biomaterials 232, 119707.
Servatan, M., Zarrintaj, P., Mahmodi, G., Kim, S.J., Ganjali, M.R., Saeb, M.R., Mozafari, M., 2020. Zeolites in drug delivery: progress, challenges and opportunities. Drug Discov. Today 25, 642–656.
Taghizadeh, A., Taghizadeh, M., Jouyandeh, M., Yazdi, M.K., Zarrintaj, P., Saeb, M.R., Lima, E.C., Gupta, V.K., 2020. Conductive polymers in water treatment: a review. J. Mol. Liq. 312, 113447.
Tavakolizadeh, M., Pourjavadi, A., Ansari, M., Tebyanian, H., Seyyed Tabaei, S.J., Atarod, M., Rabiee, N., Bagherzadeh, M., Varma, R.S., 2021. An environmentally friendly wound dressing based on a self-healing, extensible and compressible antibacterial hydrogel. Green Chem. 23, 1312–1329.
Tong, C.Y., Zhao, C., Liu, B., Li, B., Ai, Z.Y., Fan, J.L., Wang, W., 2018. Sensitive detection of RNase A activity and collaborative drug screening based on rGO and fluorescence probe. Anal. Chem. 90, 2655–2661.
Toudeshkchoui, M.G., Rabiee, N., Rabiee, M., Bagherzadeh, M., Tahriri, M., Tayebi, L., Hamblin, M.R., 2019. Microfluidic devices with gold thin film channels for chemical and biomedical applications: a review. Biomed. Microdevices 21, 93.
Vafajoo, A., Rostami, A., Foroutan Parsa, S., Salarian, R., Rabiee, N., Rabiee, G., Rabiee, M., Tahriri, M., Vashaee, D., Tayebi, L., Hamblin, M.R., 2018. Multiplexed microarrays based on optically encoded microbeads. Biomed. Microdevices 20, 1–14.
Vijayan, P., Puglia, D., Rastin, H., Saeb, M.R., Shojaei, B., Formela, K.i, 2017. Cure kinetics of epoxy/MWCNTs nanocomposites: isothermal calorimetric and rheological analyses. Prog. Org. Coat. 108, 75–83.
Wang, H.J., He, X., Luo, T.Y., Zhang, J., Liu, Y.H., Yu, X.Q., 2017. Amphiphilic carbon dots as versatile vectors for nucleic acid and drug delivery. Nanoscale 9, 5935–5947.
Wu, W.H., Hu, H.Y., Li, F., Wang, L.H., Gao, J.M., Lu, J.X., Fan, C.H., 2011. A graphene oxide-based nano-beacon for DNA phosphorylation analysis. Chem. Commun. Camb. Engl. 47, 1201–1203.
Zamani, M., Rostami, M., Aghajanzadeh, M., Kheiri Manjili, H., Rostamizadeh, K., Danafar, H., 2018. Mesoporous titanium dioxide@ zinc oxide-graphene oxide nanocarriers for colon-specific drug delivery. J. Mater. Sci. 53, 1634–1645.
Zare, H., Ahmadi, S., Ghasemi, A., Ghanbari, M., Rabiee, N., Bagherzadeh, M., Karimi, M., Webster, T.J., Hamblin, M.R., Mostafavi, E., 2021. Carbon nanotubes: smart drug/gene delivery carriers. Int. J. Nanomed. 16, 1681–1706.
Zarrintaj, P., Jouyandeh, M., Ganjali, M.R., Hadavand, B.S., Mozafari, M., Sheiko, S.S., Vatankhah-Varnoosfaderani, M., Gutiérrez, T.J., Saeb, M.R., 2019. Thermo-sensitive polymers in medicine: a review. Eur. Polym. J. 117, 402–423.
Zarrintaj, P., Khodadadi Yazdi, M., Youssefi Azarfam, M., Zare, M., Ramsey, J., Seidi, F., Mozafari, M., 2021. Injectable cell-laden hydrogels for tissue engineering: recent advances and future opportunities. Tissue Eng. doi:10.1089/ten.TEA.2020.0341.
Zarrintaj, P., Mahmodi, G., Manouchehri, S., Mashhadzadeh, A.H., Khodadadi, M., Servatan, M., Ganjali, M.R., Azambre, B., Kim, S.J., Ramsey, J.D., Habibzadeh, S., Saeb, M.R., Mozafari, M., 2020a. Zeolite in tissue engineering: opportunities and challenges.. MedComm 1, 5–34.
Zarrintaj, P., Saeb, M.R., Ramakrishna, S., Mozafari, M., 2018. Biomaterials selection for neuroprosthetics. Curr. Opin. Biomed. Eng. 6, 99–109.
Zarrintaj, P., Zangene, E., Manouchehri, S., Amirabad, L.M., Baheiraei, N., Hadjighasem, M.R., Farokhi, M., Ganjali, M.R., Walker, B.W., Saeb, M.R., Mozafari, M., Thomas, S., Annabi, N., 2020b. Conductive biomaterials as nerve conduits: recent advances and future challenges. Appl. Mater. Today 20, 100784.
Zhang, J., Wang, Z.G., Su, T.Y., Sun, H.H., Zhu, Y., Qi, Q.S., Wang, Q., 2020. Tuning the binding affinity of heme-responsive biosensor for precise and dynamic pathway regulation. iScience 23, 101067.
Zhang, Y.W., Liu, S., Sun, X.P., 2011. Mesoporous carbon microparticles as a novel fluorescent sensing platform for thrombin detection. Biosens. Bioelectron. 26, 3876–3880.
Zhao, X.H., Ma, Q.J., Wu, X.X., Zhu, X., 2012. Graphene oxide-based biosensor for sensitive fluorescence detection of DNA based on exonuclease III-aided signal amplification. Anal. Chimica Acta 727, 67–70.